An Improved Impedance Measurement Method Based on Multi-Sine Signal Considering the Suppression of Noise Interference

MENG LI[ID], HENG NIAN[ID], (Senior Member, IEEE), BIN HU[ID],
YUNYANG XU[ID], (Graduate Student Member, IEEE),
YUMING LIAO, (Graduate Student Member, IEEE), AND JUN YANG

College of Electrical Engineering, Zhejiang University, Hangzhou 310027, China

Corresponding author: Heng Nian (nianheng@zju.edu.cn)

ABSTRACT Impedance measurement is a practical method to obtain the impedance characteristic of the power electronic equipment (PEE), which is important for the small-signal stability analysis. In the impedance measurement, the measurement results may be influenced by the external noise. Therefore, it is essential to study how to avoid the measurement errors caused by the noise. To address this issue, this paper analyzes the method of suppressing the noise interference by enhancing signal-to-noise ratio (SNR) and concludes that there is limitation on improving the measurement accuracy by merely enhancing SNR due to the practical limitation on the perturbation amplitudes. And then this paper proposes an improved impedance measurement method, by which the measurement errors caused by the noise can be decreased effectively. By investigating the influence mechanism of the noise on the impedance measurement results, the measurement error can be divided into average component and fluctuant component. The average component can be eliminated by averaging two groups of measurement results with the phase difference of π rad while the influence of the fluctuant component can be minimized by employing complex-linear fitting algorithm. Finally, experiments are conducted to verify the effectiveness of proposed impedance measurement method.

INDEX TERMS Power electronic equipment, stability analysis, impedance measurement, external noise.

I. INTRODUCTION

With the rapid development and widespread application of renewable energy, the renewable power generation equipment (RPGE) has been widely utilized in power grid. Commonly, power electronic equipment (PEE) is adopted as the power interface of the power grid and RPGE. The large-scale access of the PEE into the power grid may bring about some risk of instability due to insufficient margin [1], [2]. In order to maintain the stable grid-connected operation of PEE, the small-signal stability analysis is required to evaluate the stability and guarantee sufficient stability margin.

Impedance based stability analysis is an effective method to investigate the stability of interconnected systems [3]–[6], in which the stability margin of interconnected systems can be acquired according to the impedance characteristic of the

The associate editor coordinating the review of this manuscript and approving it for publication was Xiaodong Liang[ID].

power grid and the PEE. Therefore, it is essential to acquire the accurate impedance characteristic of the PEE [7]–[10].

Impedance measurement method can obtain the impedance characteristic by injecting small-signal voltage or current perturbations into the PEE [11]–[14]. Without knowing the internal parameters of the PEE, the impedance characteristic of the PEE can be obtained according to the detected voltage and current of the injected frequency at the terminal of the PEE. Moreover, the impedance measurement can be carried out no matter whether the equipment under test is connected to the power grid. Due to the practicality and flexibility, the impedance measurement based on small-signal perturbation injection is widely adopted for impedance modeling of the PEE, Li-ion battery, passive circuit components and so on [15]–[20]. Multiple types of perturbation signals were proposed including single sine signal [15], binary sequence signal [16]–[18] and the multi-sine signal [19]. Among them, the multi-sine signal is widely adopted as the perturbation

signal which has the advantages of high measurement efficiency, controllable frequency spectrum and little spectral leakage [19].

As a matter of fact, there is noise existing in the actual PEE, which includes harmonics, switching noise and so on [21]–[23]. Thereby in the process of impedance measurement, the actual sampling signal is composed of the perturbation signal and noise signal. The existence of the noise will deteriorate the accuracy of impedance measurement results derived by the ratio of the sampling terminal voltages to currents. Overall, when the impedance characteristic of a PEE is measured based on the small-signal perturbation injection, the noise becomes a significant factor that is likely to result in measurement error. In [17], [18], the impact of the noise and signal-to-noise ratio (SNR) on the measurement results is studied. However, the method to reduce the measurement error caused by the noise is rarely discussed. A cross-correlation method has been applied in [24] and [25], by which the frequency-domain characteristic can be obtained by computing the cross-correlation between the perturbation signal and the response. However, the method performs well only on the condition that the perturbation signal is ideal white noise, which is impractical in the actual impedance measurement [24], [25].

The presence of the noise signal greatly increases the difficulty in the accurate measurement for the impedance characteristic of the PEE, which is mainly due to the variability of the frequencies, amplitudes and phases of the noise. In practice, the noise is caused by multiplex sources, which makes it difficult to identify and eliminate the influence of the noise [22], [23]. To some extent, the accuracy of the measurement results can be improved by increasing the amplitude of the perturbation signal due to the enhancement of the SNR [18], thus the influence of the external noise can be suppressed due to the increase of the proportion of the perturbation signal. However, it should be noted that there is limitation on the perturbation magnitude in the practical impedance measurement, since the SNRs cannot be increased infinitely. Therefore, while voltage perturbation injection is adopted, in the regions where the impedance magnitude is large or the noise magnitude is great, the SNR of the response signal will be unable to be guaranteed. Thereby, in the condition where the sufficient SNR is difficult to be achieved, merely increasing the perturbation amplitude may not be so effective on eliminating the effect of the noise interference. Besides, a more effective method should be adopted to improve the measurement accuracy.

In view of the above problem, an improved impedance measurement method which can effectively reduce the measurement error caused by the noise is proposed in this paper. By investigating the influence mechanism of the noise on the measurement results, the measurement error is divided into the average component and the fluctuant component. In the proposed method, both types of error components can be eliminated or decreased by two separated methods. Moreover, the combination of the two methods is also proposed in order

to effectively decrease the measurement errors caused by the noise.

This paper is organized as follows. In Section II, the impact of the SNR on the measurement accuracy is investigated by theoretical derivation and actual impedance measurement results. Additionally, the limitation on the method which reduces measurement error by enhancing SNR is presented. In Section III, by investigating the influence mechanism of the external noise on the impedance measurement results, the improved method for impedance measurement considering the suppression of the noise interference is introduced. In Section IV, experiments based on the TMS320F28335/Spartan 6 XC6SLX16 DSP + FPGA control board and Typhoon Control-hardware-in-loop (CHIL) platform are carried out for the validation of proposed method, in which the impedance characteristic of a 1.5 MW type-IV wind turbine is measured. Finally, Section V concludes this work.

II. IMPACT ANALYSIS OF SNR ON THE IMPEDANCE MEASUREMENT ACCURACY

In this section, the impact of the noise on the impedance measurement accuracy is theoretically analyzed based on the definition of SNR. In the process of impedance measurement, it is assumed that the voltage perturbation signal at the frequency of f_p Hz is injected into the PEE. In the following analysis, the noise components contained in the voltage signal and current signal at the terminal of the PEE are taken into account.

In the impedance measurement, the sampling signal at the frequency of f_p Hz contains the measurement signal and the noise components at the frequency of f_p Hz, thus the admittance measurement results can be expressed as:

$$Y_m[f_p] = \frac{I_s + I_n}{V_s + V_n} \tag{1}$$

where, I_n denotes the current noise component at the frequency of f_p Hz; V_n denotes the voltage noise component at the frequency of f_p Hz; $Y_m[f_p]$ denotes the measurement result of the admittance at the frequency of f_p Hz; V_s denotes the voltage perturbation signal at the frequency of f_p Hz; I_s denotes the current response signal at the frequency of f_p Hz.

The accurate admittance of the PEE can be expressed as:

$$Y_r[f_p] = \frac{I_s}{V_s} \tag{2}$$

where $Y_r[f_p]$ denotes the accurate admittance at the frequency of f_p Hz.

Therefore, the magnitude and phase of the admittance measurement error can be expressed as:

$$\Delta M[f_p]$$
$$= 20 \lg(|Y_m[f_p]|) - 20 \lg(|Y_r[f_p]|)$$
$$= 20 \lg(|\frac{I_s + I_n}{I_s} \times \frac{V_s}{V_s + V_n}|) \tag{3}$$
$$\Delta P[f_p] = angle(Y_m[f_p]) - angle(Y_r[f_p]) \tag{4}$$

where $\Delta M[f_p]$ represents the magnitude error of the admittance measurement result at the frequency of f_p Hz, while $\Delta P[f_p]$ represents the phase error of the admittance measurement result at the frequency of f_p Hz; $|Y_m[f_p]|$ denotes the magnitude of $Y_m[f_p]$.

In order to facilitate the analysis of the measurement error caused by the noise, the definition of SNR is introduced as:

$$\begin{cases} S_i = \frac{|I_s|}{|I_n|} \\ S_v = \frac{|V_s|}{|V_n|} \end{cases} \tag{5}$$

where S_i and S_v respectively represent the SNRs of the current signal and voltage signal. The maximum value of the $\Delta M[f_p]$ and $\Delta P[f_p]$ can be written as:

$$\Delta M_{\max} = 20\lg(\frac{S_v S_i + S_v}{S_v S_i - S_i}) \tag{6}$$

$$\Delta P_{\max} = \arcsin(1/S_v) + \arcsin(1/S_i) \tag{7}$$

According to (6)-(7), while S_v and S_i both tend to infinity, the measurement error will be equal to zero. However, if the SNR of the response signal is insufficient while the SNR of the perturbation signal is large enough, the insufficient SNR will become the dominant factor affecting the measurement accuracy and may lead to poor measurement accuracy.

Moreover, the relationship between the SNR and $\Delta M_{\max}[f_p]$ and $\Delta P_{\max}[f_p]$ is depicted in Fig. 1.
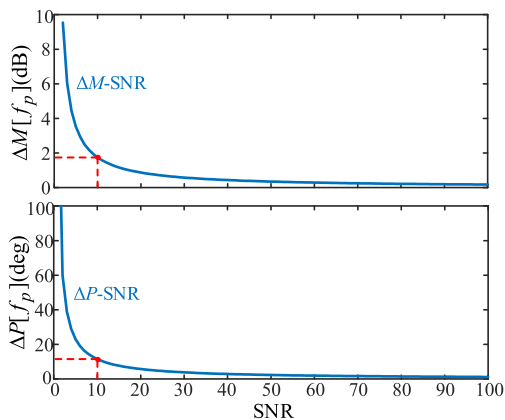

FIGURE 1. Relationship of SNR and measurement error.

According to Fig 1, with the increase of SNR, the measurement error reduces gradually in diminishing downtrend. As shown in Fig. 1, when SNR = 10, the maximum magnitude error is lower than 2 dB and the phase error is lower than 15 deg. In summary, the principle of improving the impedance measurement accuracy by enhancing the SNR is to increase the proportion of the measurement signal so that the influence of the noise signal can be weakened.

Based on the above analysis, it can be concluded that: (a) by increasing the SNR of the perturbation signal, the measurement accuracy can be enhanced effectively; (b) the sufficient SNRs of both the perturbation signal and the response signal should be guaranteed, which will both have significant

impact on the measurement accuracy. The insufficient SNR of the response signal may lead to poor measurement accuracy.

Therefore, the limitation on improving the measurement accuracy by increasing the SNR is that:

First, there is limitation on the perturbation amplitude to avoid over-modulation in the PEE under measurement, which is a nonlinear phenomenon and will result in measurement error. The amplitude limitation is mainly associated with the modulation ability and the operating point of the PEE. Thereby, the perturbation amplitudes cannot be increased infinitely.

Second, it is possible that there exist regions where the impedance magnitude is relatively great, which corresponds lower current response when the amplitude of the voltage perturbation is fixed. As a result, the sufficient SNR of the current response is difficult to be achieved considering the limitation on the perturbation magnitude. According to the above analysis, the SNR of the response signal will also impact the measurement accuracy significantly. Thus the measurement accuracy in this region is harder to be guaranteed. Besides, similar limitation also exists in other conditions. For example, in the high frequency range, due to the limited bandwidth of the perturbation generator, the perturbation strength in high frequency range is relatively weaker and thus the SNRs are also difficult to be guaranteed.

Based on the above analysis, the method of improving the measurement accuracy by enhancing SNR has obvious limitation in achieving the measurement accuracy in a wide frequency span. Accordingly, in the remaining part of this paper, by analysing the influence mechanism of the external noise on the impedance measurement results, a novel approach to decreasing the measurement error caused by the external noise is proposed, which may contribute to the accurate broadband impedance measurement of PEE.

III. IMPROVED IMPEDANCE MEASUREMENT METHOD
First of all, according to the characteristics of the external noise, the influence mechanism of the noise on the measurement results will be investigated. In [24], [25], the external noise are characterized as a signal with non-zero mean and finite variance, according to which the noise signal can be decomposed into the average component and the fluctuant component. The average component denotes the average value of the noise component which corresponds to the non-zero mean of the noise component while the fluctuant component mainly refers to the noise components which have zero mean and finite variance [25].

First, the noise component at the frequency of f_p Hz can be expressed as:

$$\begin{cases} V_n = V_e + \varepsilon_v \\ I_n = I_e + \varepsilon_i \end{cases} \tag{8}$$

where, I_n denotes the current noise component at the frequency of f_p Hz; V_n denotes the voltage noise component at the frequency of f_p Hz; I_e denotes the average component of

the current noise at the frequency of f_p Hz while ε_i denotes the fluctuant component of the current noise at the frequency of f_p Hz; V_e denotes the average component of the voltage noise at the frequency of f_p Hz while ε_v denotes the fluctuant component of the voltage noise at the frequency of f_p Hz.

According to (8), the relationship between the voltage perturbation signal and current responses can be written as:

$$I_p = Y_p V_p + \underbrace{Y_p(V_e + \varepsilon_v) + (I_e + \varepsilon_i)}_{E} \qquad (9)$$

where V_p denotes the voltage perturbation signal at the PCC (point of common coupling) at the frequency of f_p Hz; I_p denotes the current response at the frequency of f_p Hz; Y_p denotes the admittance of the PEE at the frequency of f_p Hz; E denotes the error component caused by the noise. Note that Y_p is a linear system in the impedance analysis theory, thus E can also be characterized as a component with non-zero mean and finite variance [25].

Similarly, E can be divided into the average component and fluctuant component as:

$$I_p = Y_p V_p + E_0 + \varepsilon \qquad (10)$$

According to (10), the measurement error is segmented into the average component (E_0) and fluctuant component (ε) which can be suppressed separately based on the characteristics of both types of components.

A. A METHOD FOR ELIMINATION OF E_0
According to the above definition, E_0 denotes the average component of the measurement error at the frequency of f_p Hz. The analysis on the elimination of E_0 will be introduced subsequently.

While only the average component is taken into account, the admittance measurement error can be calculated by:

$$\Delta A[f_p] = Y_r[f_p] - Y_m[f_p] = \frac{I_p}{V_p} - \frac{I_p - E_0}{V_p} = \frac{E_0}{V_p} \qquad (11)$$

where $\Delta A[f_p]$ denotes the admittance measurement error at the frequency of f_p Hz.

If the phase of the injected perturbation signal at the frequency of f_p Hz is rotated by θ rad, the measurement error can be rewritten as:

$$\Delta A_2[f_p] = \frac{E_0}{V_p} e^{-j\theta} \qquad (12)$$

The average value of $\Delta A[f_p]$ and $\Delta A_2[f_p]$ can be written as:

$$\Delta A_{aver} = \frac{1}{2}\left(\Delta A[f_p] + \Delta A_2[f_p]\right) = \frac{E_0}{2V_p}(1 + e^{-j\theta}) \qquad (13)$$

According to (13), while $\theta = \pi$ rad, $\Delta A_{aver} = 0$. It can be concluded that by averaging a pair of measurement results in which the phase difference of the perturbation signal is π rad, the error component E_0 can be eliminated.

B. METHOD FOR SUPPRESSION OF ε
According to the above definition, ε denotes the fluctuant component in the measurement error, which has zero mean and finite variance [24], [25]. In view of the random characteristic of ε, mathematical fitting algorithm is commonly used to minimize the influence of ε. According to the impedance analysis theory, the voltage perturbation and current response has linear relationship, hence, in this section a complex-linear fitting algorithm is proposed to tackle this issue [26].

Given that ε has zero mean and finite variance, for the sake of minimizing the influence of ε, an effective method is to derive the least square solution which minimizes the sum of the squares of the fitting deviation [26], [27]. Therefore, the multiple groups of measurement data should be obtained firstly, and then the least square solution of Y_p will be calculated based on groups of measurement data.

According to the above principle, in the process of impedance measurement, multiple groups of voltage perturbation signal are required to be injected into the PEE in turn and multiple groups of voltage perturbation V_p and current response I_p can be acquired. For the facilitation of depiction, the following definitions are given:

$$y = \begin{bmatrix} I_p(1) & I_p(2) & \ldots & I_p(N) \end{bmatrix}^T = [y_1 \ y_2 \ \ldots \ y_N]^T \qquad (14)$$

$$U = \begin{bmatrix} V_p(1) & V_p(2) & \ldots & V_p(N) \end{bmatrix}^T = [u_1 \ u_2 \ \ldots \ u_N]^T \qquad (15)$$

$$\boldsymbol{\varepsilon} = [\varepsilon_1 \ \varepsilon_2 \ \ldots \ \varepsilon_N]^T \qquad (16)$$

$$x = Y_p \qquad (17)$$

where N represents the number of the groups of voltage perturbation signal which are injected into the PEE; the superscript T represents matrix transpose; $I_p(i)$ $(i = 1, 2, \ldots, N)$ represents the ith group of current response; $V_p(i)$ $(i = 1, 2, \ldots, N)$ represent the ith group of voltage perturbation signal; ε_i represents the ith group of fluctuate component of the noise.

Accordingly, the relationship of I_p and V_p can be rewritten in matrix form as:

$$y = Ux + \boldsymbol{\varepsilon} \qquad (18)$$

In order to minimize the sum of the squares of the measurement error caused by the fluctuant components in the current noise, the minimum value of the following formula should be obtained as:

$$\min h = \sum_{i=1}^{N} |\varepsilon_i|^2 = \sum_{i=1}^{N} |y_i - Ux|^2 \qquad (19)$$

where h is a function regarding the real part and imaginary part of x:

$$h = h(x_r, x_i) \qquad (20)$$

In (20), x_r represents the real part of x and x_i represents the imaginary part of x. The expansion of (20) can be expressed

as:

$$h = \sum_{i=1}^{N} (y_i - u_i x) \times (\bar{y}_i - \bar{u}_i \bar{x})$$

$$= \sum_{i=1}^{N} [y_i - u_i(x_r + jx_i)] \times [\bar{y}_i - \bar{u}_i(x_r - jx_i)] \quad (21)$$

In (21), '$-$' represent the conjugate complex number. According to the least square theory [26], [27], in order to acquire the minimum value of h, the partial derivative of h with respect to x_r and x_i should both be equal to zero. Thus while (22) is satisfied, the value of x can minimize h.

$$\begin{cases} \frac{\partial h}{\partial x_r} = 0 \\ \frac{\partial h}{\partial x_i} = 0 \end{cases} \quad (22)$$

where

$$\frac{\partial h}{\partial x_r} = \sum_{i=1}^{N} [-u_i(\bar{y}_i - \bar{u}_i \bar{x}) - \bar{u}_i(y_i - u_i x)] \quad (23)$$

$$\frac{\partial h}{\partial x_i} = \sum_{i=1}^{N} [-ju_i(\bar{y}_i - \bar{u}_i \bar{x}) + j\bar{u}_i(y_i - u_i x)] \quad (24)$$

According to (23) and (24), (25) can be obtained as:

$$x \sum_{i=1}^{N} \bar{u}_i u_i = \sum_{i=1}^{N} y_i \bar{u}_i \quad (25)$$

Eq (26) can be transformed to matrix form as:

$$x = (\bar{U}^T U)^{-1} \bar{U}^T y \quad (26)$$

Therefore, the solution of Y_p which minimize h can be derived by (26). By this complex-linear fitting algorithm, the influence of the fluctuant components in the measurement error can be minimized and thereby the accuracy of the measurement results will be improved.

C. METHOD FOR THE SUPPRESSION OF THE NOISE INTERFERENCE

In A and B of this section, the methods for decreasing the average component E_0 and fluctuant components ε of the measurement error are introduced. It is noted that the intention of this paper is to decrease the measurement error composed of E_0 and ε. Therefore, the combination of both methods is proposed whose flowchart is shown in Fig. 2.

There are 5 steps contained in Fig. 2, which will be clarified in detail as follow.

(a) **Initialization:** the multi-sine signal is adopted as the perturbation signal in this paper due to the advantages of controllable frequency spectrum, high measurement efficiency and little spectral leakage [19]. The measurement frequencies should be determined according to the concerned frequency band, which can be evenly distributed in the logarithmic coordinate. Moreover, the principle for determining the amplitude of each component in the multi-sine signal is that the injection of the multi-sine signal should not influence the normal
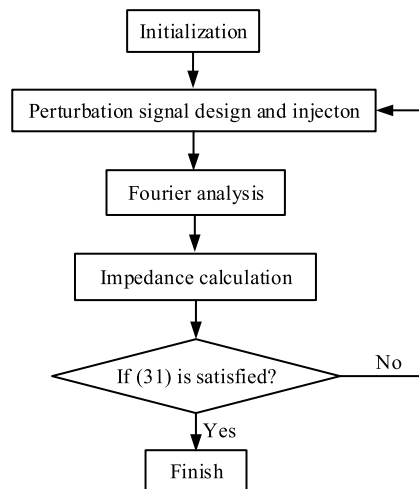

FIGURE 2. Flowchart of proposed impedance measurement method for the suppression of the noise interference.

operation of the PEE under test, which brings about limitation on the peak value of the multi-sine signal. Commonly, the injected multi-sine signal with excessive peak value will lead to over-modulation which will further influence the control of the PEE.

By (27), the margin in the modulation part of the PEE left for the multi-sine signal can be estimated by:

$$M_d = 1 - \frac{k_m |V_1 + j\omega_1 L I_1|}{V_{dc}} \quad (27)$$

where, V_1 and I_1 respectively represent the rated voltage and current of PEE; $\omega_1 = 2\pi f_1$ and f_1 is the fundamental frequency; V_{dc} is the DC-link voltage while k_m is the modulation gain and L is the filter inductance. When space vector pulse width modulation (SVPWM) is implemented,

$$k_m = \sqrt{3} \quad (28)$$

Accordingly, for the sake of avoiding over-modulation, there is limitation on the peak value of the injected multi-sine signal, which can be written as:

$$x_{peak} < M_d V_1 \quad (29)$$

In (29), x_{peak} denotes the peak value of the multi-sine signal and V_1 denotes the amplitude of V_1. In this way, an upper bound can be set for the peak value of the multi-sine signal, according to which the amplitude of each component in the multi-sine signal can be determined. Note that (29) is merely an estimation of the upper bound, therefore, additional margin could be retained if necessary.

(b) **Multi-sine signal design and injection:** in this step, a pair of multi-sine signals will be injected into the PEE in turn to implement two impedance measurements. The pair of multi-sine signals have the same amplitudes and frequency components while the phase difference of two multi-sine signals is π rad for the elimination of E_0.

(c) **Fourier analysis:** the voltage perturbation and current response signal can be obtained by applying fast Fourier

transformation (FFT) to the terminal voltages and currents of the PEE in the impedance measurement. It is noted that according to (b), two groups of voltage and current signals can be obtained after two measurements, which are respectively defined as $[V_{p_1}, I_{p_1}]$ and $[V_{p_2}, I_{p_2}]$. It is known that by averaging the measurement results calculated by $[V_{p_1}, I_{p_1}]$ and $[V_{p_2}, I_{p_2}]$, the average component (E_0) of the measurement error can be eliminated. However, in order to make it possible to simultaneously achieve the elimination of the average component and fluctuant component, a simple equivalent transformation is implemented:

$$\begin{cases} I_p = (I_{p1}V_{p2} + I_{p2}V_{p1})/\sqrt{V_{p1}V_{p2}} \\ V_p = 2\sqrt{V_{p1}V_{p2}} \end{cases} \quad (30)$$

where V_p and I_p respectively represent the equivalent voltage and current signal.

It can be seen that (30) is indeed derived by averaging a pair of admittance measurement results. Therefore, by applying the above equivalent transformation, the average component in the measurement error can be eliminated. Additionally, V_p and I_p can be used for the complex-linear fitting algorithm.

(d) **Impedance calculation:** assuming that N pairs of multi-sine signals have been injected into the PEE under test in turn, thereby N groups of $[I_p, V_p]$ can be obtained, which will be substituted into (14) and (15) to obtain y and U, and then the solution of Y_p can be derived by (26).

Overall, by applying (b)-(d), the combination of the methods for the elimination of E_0 and ε can be achieved.

(e) **Evaluation:** in the process of impedance measurement, there exists a loop to determine the value of N, which will be introduced in detail subsequently. During the loop, N will be increased gradually and the impedance measurement results can be obtained by different N.

In the ith loop ($i > 1$), the ith measurement results will be compared with the $(i-1)^{th}$ measurement results, if the following equation (31) can be met, N will not need to be increased furtherly. Otherwise, step (b)-(d) will be repeated. The difference between the two adjacent loops is that the number of $[I_p, V_p]$ used in impedance calculation is different: in the ith loop, $N = i$ while in the $(i-1)^{th}$ loop, $N = i - 1$. The loop will be ended until (31) can be satisfied.

$$\begin{cases} \max\left[20\lg(|Z^{(i)}|) - 20\lg(|Z^{(i-1)}|)\right] < D_a \\ \max\left[angle\left(Z^{(i)} - Z^{(i-1)}\right)\right]/\pi \times 180 < D_p \end{cases} \quad (31)$$

In (31), D_a (dB) and D_p (deg) respectively denote the threshold values for the magnitude and phase of the measurement results. $Z^{(i)}$ denotes the measurement results obtained when $N = i$ and $Z^{(i-1)}$ denotes the measurement results obtained when $N = i - 1$.

IV. EXPERIMENTS VERIFICATION OF PROPOSED IMPEDANCE MEASUREMENT METHOD

In order to further verify the effectiveness of the proposed impedance measurement method for the decrease of the measurement error caused by the noise, the experiments based
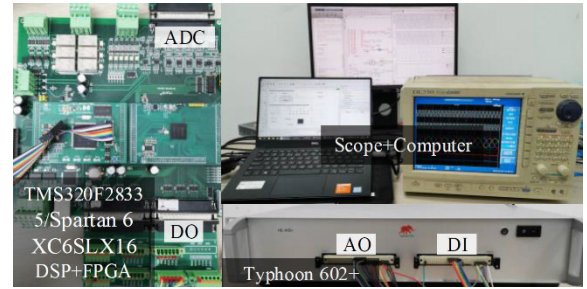

FIGURE 3. Hardware platform of typhoon CHIL experiment.

on Control-hardware-in-loop (CHIL) are carried out. The hardware platform of CHIL experiment is shown in Fig. 3. The model of a 1.5 MW type-IV wind turbine is developed in Typhoon 602 + whose impedance characteristic in 1 ~ 1000 Hz will be measured. Controllers of the type-IV wind turbine and the perturbation generator are implemented in the control board. There are signal conditioning circuits in the control board. By analog/digital convertion (ADC), the circuit signals can be received by the control board and then utilized for the generation of the switching signal, which can be output by the digital output (DO) ports of the control board. Furthermore, by the analog output (AO) ports and the digital input (DI) ports, the Typhoon 602 + platform can implement the output of circuit signals and receive the swithing signal from the control board. It should be noted that the external noise introduced by the voltage/current sensors in the real prototype is the main factor which may interfere the measurement precision [15]–[20]. Therefore, in order to emulate the noise brought about by the sensors, a noise generator is adopted to generate random noise signal which will be superimposed with the voltage and current signals [25], [28].

The parameters of the type-IV wind turbine are shown in Table 1.

TABLE 1. Partial parameters of the type-IV wind turbine under test.

Symbol	Parameter	Value
U_s	Rated voltage	690 V
P_s	Rated power	1.5 MW
f_s	Switching frequency	5 kHz
f_1	Fundamental frequency	50 Hz
V_{dc}	Dc-link voltage	1100 V
L	Filter inductance	0.4 mH
k_{pp}	Proportional gain of PLL controller	44
k_{pi}	Integral gain of PLL controller	500
k_{ip}	Proportional gain of current controller	3.35
k_{ii}	Integral gain of current controller	315

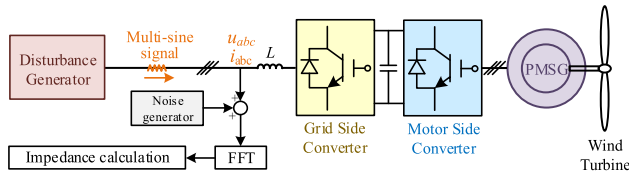In this paper, the schematic of the impedance measurement system is shown in Fig. 4.

FIGURE 4. Schematic of the impedance measurement system.

According to Fig. 4, the perturbation generator is connected in series with the type-IV wind turbine, which can inject perturbation signal into the type-IV wind turbine for impedance measurement while maintaining the normal operation of the type-IV wind turbine. In the impedance measurement, the external noise is respectively superimposed with the voltage perturbation signal and current response signal which will bring about interference to the measurement accuracy. Under the interference of the external noise, the positive-sequence admittance of the wind turbine in the range of $1 \sim 1000$ Hz are measured by the injection of multi-sine signal.

First, the amplitudes and phases of individual components of the multi-sine signal should be determined. The amplitudes of each component can be selected to be the same considering the control capability of the perturbation generator [20]. The phases of each component can be determined by clipping method proposed in [19] and the amplitude can be designed by means of proposed method presented in (27)-(29). According to the parameters of the type-IV wind turbine the upper bound for the peak value of the multi-sine signal can be derived by (27)-(29). Therefore, the amplitude of each component in the multi-sine signal can be determined as 5 V. The average amplitude of the external voltage noise generated by the noise generator is about 1 V. Accordingly, the SNR of the perturbation signal is 5. According to the analysis in Section II, such SNR level will possibly lead to the measurement error exceeding 3 dB and 20 deg.

During the process of impedance measurement, the three-phase line-to-line voltages at PCC (U_{PCC}), output currents (I_{abc}) and the output active (P_o) and reactive power (Q_o) of the type-IV wind turbine are shown in Fig. 5, which indicates that the normal operation of the type-IV wind turbine can be maintained when the perturbation signal is injected into the type-IV wind turbine merely the multi-sine signal is superimposed. Moreover, when the perturbation signal is disabled, the operation of wind turbine can still return to the normal state.

In order to avoid over-modulation, the perturbation amplitudes are 5 V. For the sake of revealing the limitation on the perturbation amplitudes, the measurement results obtained while perturbation amplitudes are 10 V are shown in Fig. 6. In order to reveal the accuracy of the measurement results, the admittance obtained by frequency scan is presented as a reference [28], which is depicted by the red solid lines.

According to Fig. 6, the average magnitude error is 3.7 dB and the maximum magnitude error is 14 dB, which indicates
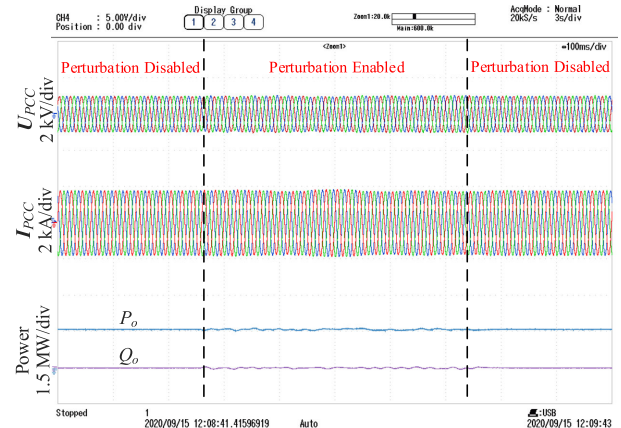

FIGURE 5. Experimental results of the voltages at PCC, output currents and output power of the type-IV wind turbine with the injection of perturbation signal.
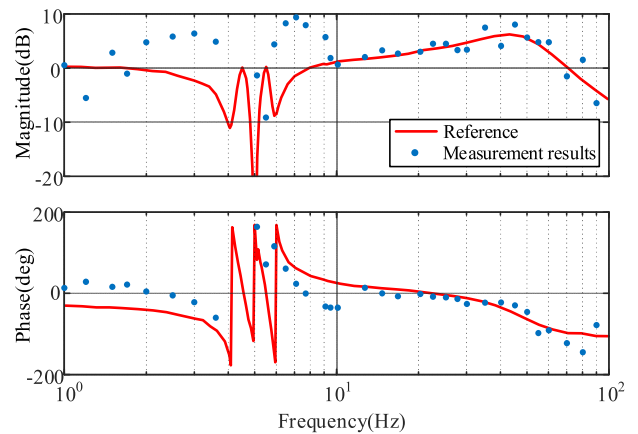

FIGURE 6. Measurement results under over-modulation.

that the measurement accuracy is poor since the measurement points are seriously deviated from the reference admittance. The reason is that the peak value of the perturbation signal has exceeded the upper-limit of the modulation part in PEE. Therefore, the perturbation amplitudes cannot be increased infinitely to avoid over-modulation.

In the following, the measurement results of the positive-sequence admittance obtained by single injection are shown in Fig. 7, in which the red solid line denotes the actual admittance obtained by frequency scan based on the injection of single sine signal [15] while blue dots denote the measurement results.

As shown in Fig. 7, The average magnitude error is 1.50 dB and the maximum magnitude error is 7.5 dB, revealing that the measurement accuracy is poor, which is mainly caused by the noise interference. It should be indicated that the measurement error in high frequency range ($500 \sim 1000$ Hz) are more significant since the perturbation amplitudes in high frequency range become weak.

Moreover, in [17], the method of decreasing the error caused by the noise is proposed in which the average value of multiple groups of measurement results are obtained so as to reduce the effect of the noise. In order to investigate
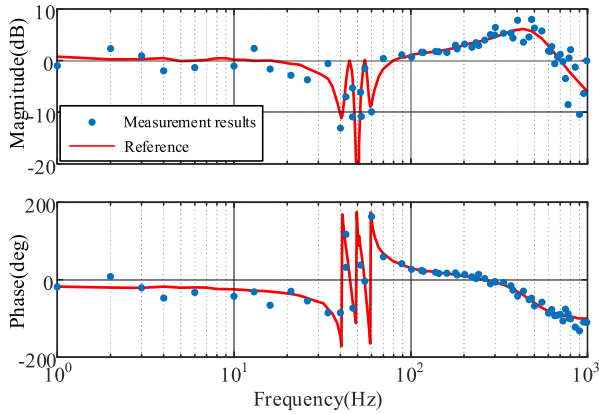
FIGURE 7. The measurement results obtained by single injection.
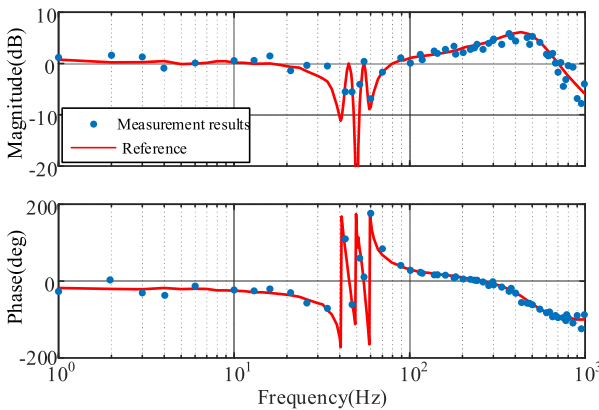

FIGURE 8. The measurement results obtained by averaging.

the performance of the method proposed in [17], the results obtained by averaging 12 groups of measurement results of are shown in Fig. 8. According to the results in Fig. 8, the average magnitude error is 1.01 dB and the maximum magnitude error is 4.3 dB, which indicates that the accuracy has been improved after averaging 12 groups of measurement results whereas there is still obvious error. Due to the fluctuation of the noise, to some extent the positive and negative error can cancel each other out by averaging. However, the average component of the noise is unable to be eliminated by merely averaging multiple groups of measurement results obtained by the same multi-sine signal, hence the errors caused by the noise is difficult to be decreased effectively by this way.

In order to validate the effectiveness of the proposed impedance measurement method, the process in Fig. 2 is implemented to obtain measurement results. In this paper, $D_a = 0.5$ dB and $D_p = 5$ deg. Finally, (31) is met until $N = 6$. Therefore, the results obtained while $N = 6$ are presented as the final measurement results of proposed method. Thereby 6 pairs of multi-sine signal are injected into the type-IV wind turbine under test in turn. The phase difference of a pair of multi-sine signals is π rad, whose amplitude-frequency and phase-frequency characteristics are depicted in Fig. 9.

The results obtained by averaging only a pair of measurement results are shown in Fig. 10. According to the results
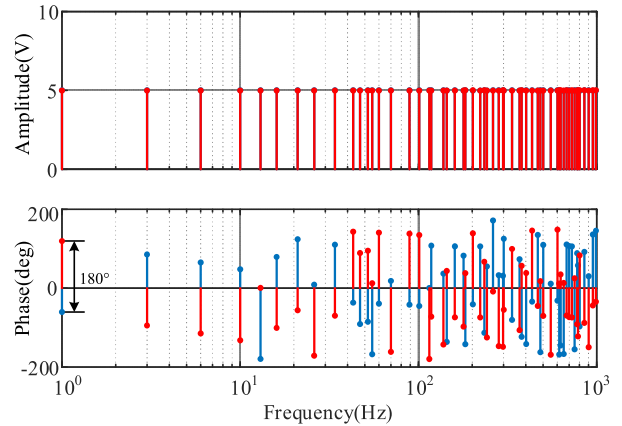
shown in Fig. 10, the average magnitude error is 1.26 dB and the maximum magnitude error is 5.8 dB.

According to Fig. 10, compared with the results in Fig. 7, the measurement accuracy is improved after averaging a pair of measurement results with the phase difference of π rad whereas there are still considerable errors, which is mainly due to that only the average component (E_0) can be decreased. Due to the variability of the external noise, the fluctuant component is also required to be handled.

FIGURE 9. The amplitude-frequency and phase-frequency characteristic of a pair of multi-sine signal with 180 deg phase difference.
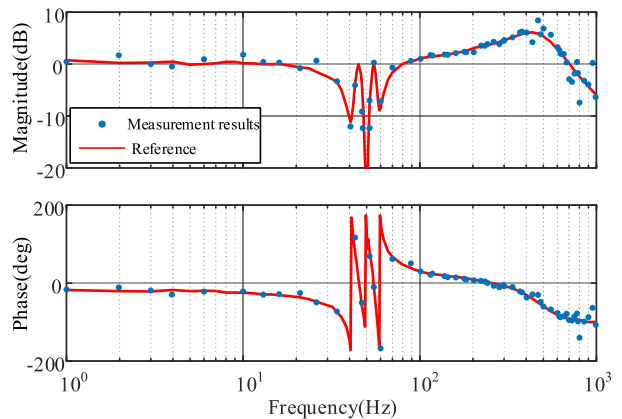

FIGURE 10. The measurement results obtained by a pair of measurement results with the phase difference of 180 deg.

Subsequently proposed method presented in Section III is applied based on 6 pairs of voltage perturbation signals and current responses, and then the accurate measurement results can be obtained, which are shown in Fig. 11, according to which, the average magnitude error is 0.35 dB and the maximum magnitude error is 1.91 dB. Therefore, it can be indicated that the measurement accuracy has been obviously enhanced compared with the results obtained by single injection and averaging method [17], which concludes that the average component and fluctuant component of the error can be both decreased effectively by proposed method.
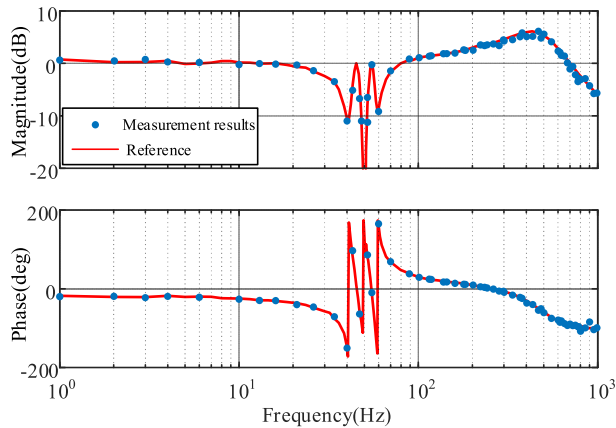
FIGURE 11. The measurement results obtained by proposed method.

V. CONCLUSION

Considering the interference from the external noise in the impedance measurement of the PEE, an improved impedance measurement method is proposed to decrease the measurement errors caused by the noise. The average components and the fluctuant components in the measurement error can be decreased respectively by averaging groups of measurement results where the phase difference of the multi-sine signals is π rad and applying complex-linear fitting algorithm. Finally, the effectiveness of proposed method is validated by experiments based on Typhoon CHIL platform. The experimental results reveal that the proposed method has excellent impedance measurement accuracy under the interference of the external noise.

REFERENCES

[1] M. Cespedes and J. Sun, "Mitigation of inverter-grid harmonic resonance by narrow-band damping," *IEEE J. Emerg. Sel. Topics Power Electron.*, vol. 2, no. 4, pp. 1024–1031, Dec. 2014.

[2] X. Wang and F. Blaabjerg, "Harmonic stability in power electronic-based power systems: Concept, modeling, and analysis," *IEEE Trans. Smart Grid*, vol. 10, no. 3, pp. 2858–2870, May 2019.

[3] J. Sun, "Impedance-based stability criterion for GCIs," *IEEE Trans. Power Electron.*, vol. 26, no. 11, pp. 3075–3078, Nov. 2011.

[4] J. Sun, "Small-signal methods for AC distributed power systems—A review," *IEEE Trans. Power Electron.*, vol. 24, no. 11, pp. 2545–2554, Nov. 2009.

[5] B. Wen, D. Boroyevich, R. Burgos, P. Mattavelli, and Z. Shen, "Analysis of D-Q small-signal impedance of grid-tied inverters," *IEEE Trans. Power Electron.*, vol. 31, no. 1, pp. 675–687, Jan. 2016.

[6] M. Cespedes and J. Sun, "Impedance modeling and analysis of grid-connected voltage-source converters," *IEEE Trans. Power Electron.*, vol. 29, no. 3, pp. 1254–1261, Mar. 2014.

[7] I. Vieto and J. Sun, "Sequence impedance modeling and analysis of type-III wind turbines," *IEEE Trans. Energy Convers.*, vol. 33, no. 2, pp. 537–545, Jun. 2018.

[8] Y. Xu, H. Nian, T. Wang, L. Chen, and T. Zheng, "Frequency coupling characteristic modeling and stability analysis of doubly fed induction generator," *IEEE Trans. Energy Convers.*, vol. 33, no. 3, pp. 1475–1486, Sep. 2018.

[9] X. Wang, F. Blaabjerg, and W. Wu, "Modeling and analysis of harmonic stability in an AC power-electronics-based power system," *IEEE Trans. Power Electron.*, vol. 29, no. 12, pp. 6421–6432, Dec. 2014.

[10] I. Vieto and J. Sun, "Refined small-signal sequence impedance models of type-III wind turbines," in *Proc. IEEE Energy Convers. Congr. Expo. (ECCE)*, Sep. 2018, pp. 1–8.

[11] T. Roinila, T. Messo, R. Luhtala, R. Scharrenberg, E. C. W. de Jong, A. Fabian, and Y. Sun, "Hardware-in-the-loop methods for real-time frequency-response measurements of on-board power distribution systems," *IEEE Trans. Ind. Electron.*, vol. 66, no. 7, pp. 5769–5777, Jul. 2019.

[12] T. Roinila, H. Abdollahi, S. Arrua, and E. Santi, "Real-time stability analysis and control of multiconverter systems by using MIMO-identification techniques," *IEEE Trans. Power Electron.*, vol. 34, no. 4, pp. 3948–3957, Apr. 2019.

[13] J. P. Rhode, A. W. Kelley, and M. E. Baran, "Complete characterization of utilization-voltage power system impedance using wideband measurement," *IEEE Trans. Ind. Appl.*, vol. 33, no. 6, pp. 1472–1479, Dec. 1997.

[14] M. Nagpal, W. Xu, and J. Sawada, "Harmonic impedance measurement using three-phase transients," *IEEE Trans. Power Del.*, vol. 13, no. 1, pp. 272–277, Feb. 1998.

[15] J. Castello and J. M. Espi, "DSP implementation for measuring the loop gain frequency response of digitally controlled power converters," *IEEE Trans. Power Electron.*, vol. 27, no. 9, pp. 4113–4121, Sep. 2012.

[16] J. Sihvo, D.-I. Stroe, T. Messo, and T. Roinila, "A fast approach for battery impedance identification using pseudo random sequence (PRS) signal," *IEEE Trans. Power Electron.*, vol. 35, no. 3, pp. 2548–2557, Jul. 2019.

[17] T. Roinila, M. Vilkko, and J. Sun, "Broadband methods for online grid impedance measurement," in *Proc. IEEE Energy Convers. Congr. Expo.*, Sep. 2013, pp. 3003–3010

[18] T. Roinila, M. Vilkko, and J. Sun, "Online grid impedance measurement using discrete-interval binary sequence injection," *IEEE J. Emerg. Sel. Topics Power Electron.*, vol. 2, no. 4, pp. 985–993, Dec. 2014.

[19] H. Zappen, F. Ringbeck, and D. Sauer, "Application of time-resolved multi-sine impedance spectroscopy for lithium-ion battery characterization," *Batteries*, vol. 4, no. 4, p. 64, Dec. 2018.

[20] H. Hu, P. Pan, Y. Song, and Z. He, "A novel controlled frequency band impedance measurement approach for single-phase railway traction power system," *IEEE Trans. Ind. Electron.*, vol. 67, no. 1, pp. 244–253, Jan. 2020.

[21] A. Testa, M. F. Akram, R. Burch, G. Carpinelli, G. Chang, V. Dinavahi, C. Hatziadoniu, W. M. Grady, E. Gunther, M. Halpin, and P. Lehn, "Interharmonics: Theory and modeling," *IEEE Trans. Power Del.*, vol. 22, no. 4, pp. 2335–2348, Oct. 2007.

[22] H. Soltani, P. Davari, F. Zare, and F. Blaabjerg, "Effects of modulation techniques on the input current interharmonics of adjustable speed drives," *IEEE Trans. Ind. Electron.*, vol. 65, no. 1, pp. 167–178, Jan. 2018.

[23] H. Soltani, P. Davari, F. Zare, P. C. Loh, and F. Blaabjerg, "Characterization of input current interharmonics in adjustable speed drives," *IEEE Trans. Power Electron.*, vol. 32, no. 11, pp. 8632–8643, Nov. 2017.

[24] B. Johansson and M. Lenells, "Possibilities of obtaining small-signal models of DC-to-DC power converters by means of system identification," in *Proc. 22nd Int. Telecommun. Energy Conf. INTELEC*, Sep. 2000, pp. 65–75.

[25] A. Barkley and E. Santi, "Improved online identification of a DC–DC converter and its control loop gain using cross-correlation methods," *IEEE Trans. Power Electron.*, vol. 24, no. 8, pp. 2021–2031, Aug. 2009.

[26] H. Hua, X. Jia, D. Cao, and C. Zhao, "Practical method to determine the harmonic contribution of a specific harmonic load," in *Proc. IEEE 15th Int. Conf. Harmon. Qual. Power*, Jun. 2012, pp. 769–773.

[27] M. S. Spurbeck and C. T. Mullis, "Least squares approximation of perfect reconstruction filter banks," *IEEE Trans. Signal Process.*, vol. 46, no. 4, pp. 968–978, Apr. 1998.

[28] H. Nian, M. Li, B. Hu, L. Chen, and Y. Xu, "Design method of multi-sine signal for broadband impedance measurement," *IEEE J. Emerg. Sel. Topics Power Electron.*, early access, Jan. 18, 2021, doi: 10.1109/JESTPE.2021.3052220.
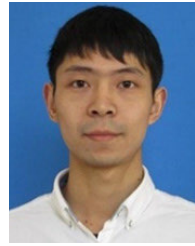
MENG LI was born in Chifeng, China. He received the B.Eng. degree in electrical engineering from Zhejiang University, Hangzhou, China, in 2019, where he is currently pursuing the Ph.D. degree in electrical engineering.

His research interests include small-signal stability analysis of grid-connected operation and the technology for impedance measurement of renewable generators.

HENG NIAN (Senior Member, IEEE) received the B.Eng. and M.Eng. degrees in electrical engineering from the Hefei University of Technology, China, in 1999 and 2002, respectively, and the Ph.D. degree in electrical engineering from Zhejiang University, China, in 2005, respectively.

From 2005 to 2007, he held a postdoctoral position with the College of Electrical Engineering, Zhejiang University, where he was promoted to an Associate Professor, in 2007. Since 2016, he has been a Full Professor with the College of Electrical Engineering, Zhejiang University. From 2013 to 2014, he was a Visiting Scholar with the Department of Electrical, Computer, and System Engineering, Rensselaer Polytechnic Institute, Troy, NY, USA. He has published more than 40 IEEE/IET transaction articles and holds more than 20 issued/pending patents. His current research interests include the optimal design and operation control for wind power generation systems.

BIN HU was born in Wenzhou, China. He received the B.Eng. degree in electrical engineering from the Shenyang University of Technology, Shenyang, China, in 2018. He is currently pursuing the Ph.D. degree in electrical engineering with Zhejiang University.

His research interests include impedance characteristic analysis and reshaping method for wind power generation systems.

YUNYANG XU (Graduate Student Member, IEEE) was born in Deyang, China. She received the B.Eng. degree in electrical engineering from Zhejiang University, Hangzhou, China, in 2016, where she is currently pursuing the Ph.D. degree in electrical engineering.

Her research interests include small-signal modeling of renewable generators and their integration to the electric grid and system stability analysis.

YUMING LIAO (Graduate Student Member, IEEE) was born in Ganzhou, Jiangxi, China. He received the M.Eng. degree in electronics and power transmission from the Department of Electrical Engineering, Hefei University of Technology, Hefei, China, in 2018. He is currently pursuing the Ph.D. degree in electrical engineering with Zhejiang University, Hangzhou, China.

His research interests include stability analysis of grid-connected operation and wind power generation systems.
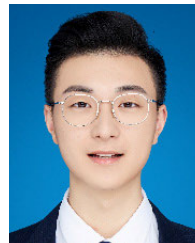
JUN YANG was born in Wenzhou, China. He received the B.Eng. degree in electrical engineering from Zhejiang University, Hangzhou, China, in 2019, where he is currently pursuing the M.Eng. degree in electrical engineering.

His research interests include the impedance-based stability analysis methods for ac/dc hybrid power system under weak ac grid and corresponding impedance reshaping control strategy.

$\bullet\ \bullet\ \bullet$